

Synthesis of Zn-Fe Nanoparticles Using Pulse Laser Ablation as a Contrast Agent in Magnetic Resonance Imaging

by Eko Hidayanto

Submission date: 12-May-2022 01:49PM (UTC+0700)

Submission ID: 1834452075

File name: C27.pdf (1.14M)

Word count: 3761

Character count: 19410

Journal of Physics and Its Applications

Journal homepage :<https://ejournal2.undip.ac.id/index.php/jpa/index>



Synthesis of Zn-Fe Nanoparticles Using Pulse Laser Ablation as a Contrast Agent in Magnetic Resonance Imaging

Nurul Hikmantiyah, Eko Hidayanto, and Ali Khumaeni*

Department of Physics, Faculty of Science and Mathematics, Diponegoro University, Jl. Prof. Soedharto, SH., Tembalang, Semarang 50275, Indonesia
*corresponding author: khumaeni@fisika.fsm.undip.ac.id

ARTICLE INFO

Article history:

Received : 25 November 2019

Accepted : 7 December 2019

Available online : 10 December 2019

Keywords:

Pulse laser ablation

Zinc oxide nanoparticles

Zn-Fe nanoparticles

MRI contrast agent

ABSTRACT

Synthesis of zinc oxide nanoparticles, iron oxide nanoparticles and Zn-Fe nanoparticles using pulse laser ablation method has been conducted. Experimentally, a pulse Nd:YAG laser (1064 nm, 7 ns, 35 mJ) was directed and focused on a metal plates of pure Zn and Fe, which are placed in the liquid medium of polyvinyl pyrrolidone (PVP). The PVP functions as a stabilizer agent. The results show that the produced nanoparticles have a spherical shape with an averaged diameter of Zn-Fe nanoparticles of 13 nm. FTIR and XRD test results of Zn-Fe nanoparticles show characteristics of Zn-Fe compounds. The examination of Zn-Fe nanoparticles as MRI contrast agents was carried out by varying the concentration of nanoparticles. Cen calculation results showed the highest contrast enhancement occurred at a concentration of 1.25 mM with a value of 64.26% for T1 weighted images, and 81.52% for T2 weighted images. The SNR calculation results show the highest value at a concentration of 1.25 mM of 70.52 for T1 weighted images. The highest SNR value in the T2 weighted image at a concentration of 0.156 mM of 165.09.

1. Introduction

The development of medical imaging technology has been increasingly rapid and sophisticated. One of the medical imaging technologies used recently is Magnetic Resonance Imaging (MRI), which can produce three-dimensional (3D) images of the body. Although it is said to be sophisticated, in MRI imaging technology, there are still many challenges that must be faced so that the diagnosis is more accurate, such as taking into account the presence of various artifacts (air bubbles, calcification) or limited sensitivity [1]. In addition, it is quite difficult to distinguish tissue with almost the same density so that this can interfere with the diagnosis process. The application of contrast agents makes it possible to eliminate some of these problems. Contrast agents have an important role by increasing the contrast between normal and abnormal tissue. By improving image quality, organs with almost the same density can be clearly distinguished thereby increasing MRI sensitivity [2, 3].

Nanomaterials have good potential in the field of medical diagnosis. Nanoparticles (NP) as contrast agents are promising strategies for noninvasive diagnosis based on the results of *in vivo* and *in vitro* tests that have been carried out [4]. So far, the contrast agent that is commonly used in MRI is gadolinium. However, the results of recent research indicate that gadolinium can harm the body because it accumulates in the brain and other body tissues [5].

Research in recent years shows that iron nanoparticles have good potential to be used as an

MRI contrast agent. This relates to superparamagnetic properties, biodegradability, and surfaces that are easily modified with biocompatible coatings [6, 7]. Iron nanoparticles have been shown to improve image quality based on *in vitro* and *in vivo* test results with low toxicity values, with 90% cells remaining for 24 hours at high concentrations of 100 $\mu\text{g mL}^{-1}$ iron [8]. Iron nanoparticles can be combined with zinc because of lower Zn + toxicity. Zn-Fe nanoparticles are good candidates for MRI contrast agents because the allowable dose of RDI (Reference Daily Intake) for iron and zinc are 18 and 15 mg days respectively, which is much higher than other biocompatible materials [9, 10].

Several chemical methods have been used for the synthesis of Zn-Fe nanoparticles, including the hydrothermal method [11], precipitation method [12], and combustion method [13], but the methods require complicated procedures and require chemicals as surfactants. Furthermore, this causes the nanoparticles produced to have low purity so that it is not appropriate to be applied in the health field. Another method used for nanoparticle synthesis is pulse laser ablation. In this method a high-power pulse laser is focused on the metal surface placed in the liquid to produce colloidal nanoparticles. Compared to chemical methods, the laser ablation method does not require complicated processes, is environmentally friendly, and high purity nanoparticles can be produced because they do not require surfactants in the synthesis process [14]. The laser ablation process of pulses on the metal surface of zinc and iron will induce the formation of

1 zinc and iron nanoparticle colloids without the use of organic surfactants, so that nanoparticles with high purity are produced [15, 16]. However, in those researchs, high energy of laser pulse was used and the liquid used as the medium is pure water.

In this present work, synthesis of Zn-Fe nanoparticles were made using pulse laser ablation method utilizing a pulse Nd:YAG laser with a quite laser energy of 35 mJ in the pure water and polyvinyl pyrrolidone (PVP) as liquid medium. The nanoparticles were then characterized to obtain information on morphology, size distribution, and elemental composition. The Zn-Fe nanoparticles were then applied as a contrast agent in MRI.

2. Experimental procedure

Experimental setup used in this work is shown in Fig. 1. A pulse Nd:YAG laser (1064 nm, 7 ns, 35 mJ) was irradiated and focused on a high purity metal plate of Zn and Fe, which were placed and immersed in a aquades or PVP medium. The pulse laser used 10 repetition rate during data acquisition. A luminous plasma was then produced just on the surface of metal plate and finally diminished and dispersed into the aquades to produce colloidal nanoparticles.

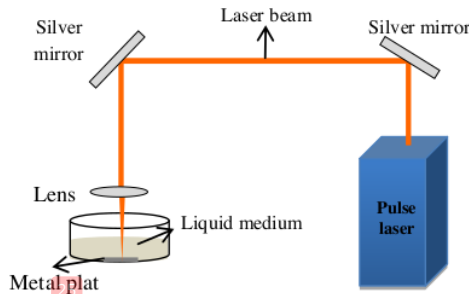


Fig. 1: Experimental setup used in this work.

To produce colloidal Zn-Fe nanoparticles, colloidal zinc nanoparticles were firstly synthesized from the Zinc metal plate. The synthesis of colloidal Fe nanoparticles was subsequently produced from the Fe metal plate. Finally, the colloidal Zn and Fe nanoparticles were mixed, and the laser beam was focused on the mixture to produce colloidal Zn-Fe nanoparticles.

2 The produced colloidal Zn, Fe, and Zn-Fe nanoparticles were then characterized by using SEM-EDX, TEM, UV-Vis, and FTIR to obtain morphology, size distribution, and elemental composition of colloidal nanoparticles.

3. Results and discussion

3.1 Syntesis of colloidal zinc oxide nanoparticles in pure water and PVP

First, syntesis of colloidal zinc oxide nanoparticles in aquades and PVP was performed. Zinc oxide nanoparticles were synthesized using a Nd: YAG pulse laser with an energy of 35 mJ, a repetition rate of 10 Hz at a wavelength of 1064 nm and a pulse width of 7 ns. The ablation process was carried out for 80 minutes. Figure 2(a) and 2(b) shows colloidal zinc oxide nanoparticles in pure water and 0.5 mM PVP medium, respectively. It can

be observed that there is a color difference between colloidal zinc oxide nanoparticles synthesized in distilled water and PVP. The colloidal zinc nanoparticles synthesized in pure water medium have a brownish yellow color and are cloudy, while the colloidal zinc in the PVP medium is much clearer. The zinc oxide nanoparticles that are formed are highly reactive and tend to react with the surrounding environment, and react with each other so that they are easily agglomerated. In the PVP medium the agglomeration process can be reduced, because the PVP liquid which is a polymer will coat the outer surface of the zincoxide nanoparticles thereby limiting their interaction with the surrounding environment. Therefore, the use of PVP as a liquid medium can produce a good stability of colloidal nanoparticles. The addition of PVP as a stabilizer produces zinc oxide monodispersion nanoparticles and prevents agglomeration.

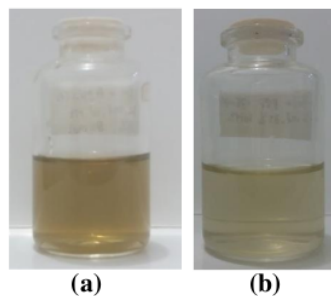


Fig. 2: Colloidal zinc oxide nanoparticles in (a) pure water and (b) PVP.

27 Figure 3 shows absorption spectrum of colloidal zinc oxide nanoparticles in pure water (blue line) and PVP (red line). It is observed that the full width of half maximum of the spectrum of the zinc oxide nanoparticle colloid in the PVP medium is much narrower compared to the spectrum of the colloidal zinc oxide nanoparticle in a pure water. The narrower spectrum shows that the produced nanoparticles have a smaller size, while the wide peak is an indication of the formation of large particles and the possibility of agglomeration. This result will be further proven by calculating the size distribution of zinc oxide nanoparticles in pure water and PVP.

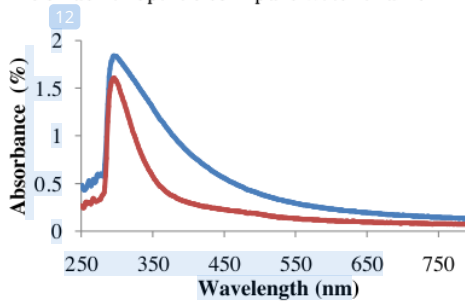


Fig. 3: Absorption spectrum of colloidal zinc oxide nanoparticles in pure water (blue line) and PVP (red line).

Figure 4 shows the colloidal morphology of zinc oxide nanoparticles in the aquades medium and 5 mM PVP.

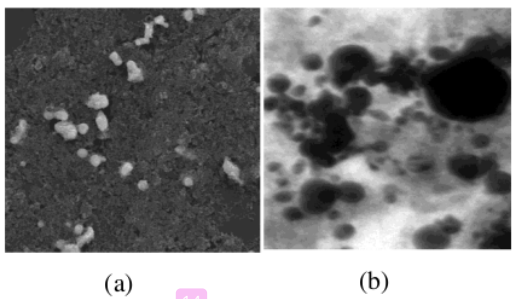


Fig. 4: SEM image of zinc oxide nanoparticles produced in (a) pure water and (b) PVP medium.

In this study the results of SEM images of zinc oxide colloidal nanoparticles in pure water were compared with the results of TEM colloidal zinc oxide nanoparticles in PVP medium. The image from SEM observation can only show the surface morphology of the sample so that it is very difficult to penetrate the PVP layer that overlaps the zinc oxide nanoparticles. For this reason, the zinc oxide nanoparticles in the PVP is measured by TEM. Based on Figs. 4(a) and 4(b), zinc oxide nanoparticles synthesized in aqueous and PVP medium have a spherical shape. This result is in accordance with the results of UV-Vis analysis with both samples having a single peak. The SEM and TEM analysis results in Figure 4 are then processed using imageJ software to obtain the nanoparticle size distribution.

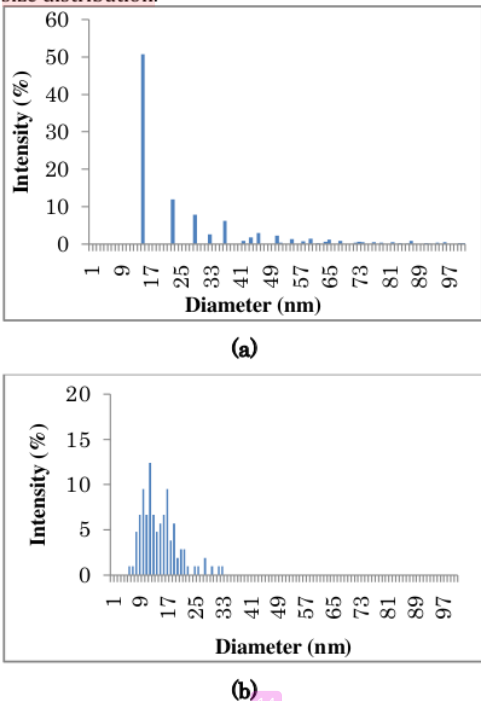


Fig. 5: Size distribution of zinc oxide nanoparticles produced in (a) pure water and (b) PVP medium.

Figure 5 shows the distribution of zinc oxide particles histograms in pure water and PVP at 35 mJ laser energy. From the calculation results obtained zinc oxide nanoparticles synthesized with distilled

water medium has an average diameter of 28 nm, while zinc oxide nanoparticles synthesized in PVP medium have an average diameter of 11 nm. Based on these values it can be seen that zinc oxide nanoparticles synthesized in PVP medium have a smaller average diameter. This is because the addition of PVP can reduce the agglomeration of zinc oxide nanoparticles.

3.2 Synthesis of iron oxide nanoparticles in PVP medium

Synthesis of iron oxide nanoparticles by pulse laser ablation method has been carried out. Synthesis of iron oxide nanoparticles was carried out at 35 mJ laser energy, a repetition rate of 10 Hz, and a pulse width of 7 ns in a 5 mM PVP medium. 35 mJ laser energy was chosen because it is considered the most optimal, lower laser energy produces nanoparticles with small concentrations so that it takes longer ablation time, while laser energy that is too high can produce nanoparticles with high concentrations quickly but nanoparticles produced are very easy to experience agglomeration. 5 mM PVP medium is used in the synthesis of iron oxide nanoparticles to produce stable colloidal iron oxide nanoparticles. Colloidal iron oxide nanoparticles are shown in Fig. 6. Based on these images it can be observed that colloidal iron oxide nanoparticles have a reddish yellow color.



Fig. 6: Colloidal iron oxide nanoparticles produced in PVP medium.

Morphological features of iron oxide nanoparticles were obtained using TEM devices. TEM images are then used to calculate the size distribution of iron oxide nanoparticles by utilizing the imageJ software. Morphological description of iron oxide nanoparticles and histogram of the size distribution of nanoparticles are shown in Fig. 7. It can be observed that iron oxide nanoparticles synthesized using the laser ablation method in the PVP medium have a spherical shape. In addition, the synthesis of iron oxide nanoparticles in a 5 mM PVP medium produces small sized iron oxide nanoparticles with a diameter of 4 nm.

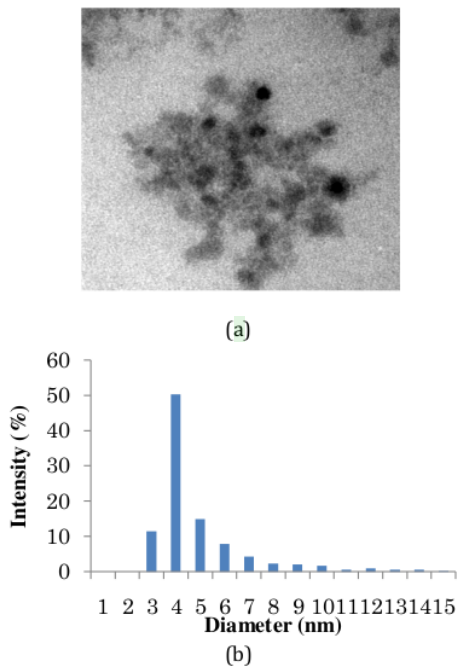


Fig. 7: (a) TEM image of colloidal iron oxide nanoparticles produced in PVP medium, and (b) size distribution of iron oxide nanoparticles.

3.3. Synthesis of colloidal Zn-Fe nanoparticles

In the synthesis of Zn-Fe nanoparticles, the PVP medium was used to produce nanoparticles that are stable and not easily agglomerated. To make a mixture of colloidal nanoparticles, colloidal zinc oxide nanoparticles in the PVP medium were mixed with colloidal iron oxide nanoparticles in a PVP medium. The synthesis parameters for iron oxide nanoparticles are the same as the parameters used in the synthesis of zinc oxide and iron oxide nanoparticles, namely 35 mJ laser energy and laser repetition rate of 10 Hz. The mixture was stirred with an ultrasonic bedge to obtain a homogeneous mixture. The mixture was then irradiated by a laser beam for 6 hours.



Fig. 8: Colloidal nanoparticles of (a) zinc oxide, (b) iron oxide nanoparticles, and (c) mixture of Zn-Fe.

Figure 8 shows colloidal zinc oxide nanoparticles, iron oxide nanoparticles, and Zn-Fe nanoparticles. It

is seen that colloidal zinc and iron nanoparticles have orange color due to the mixing of clear zinc oxide nanoparticles with reddish yellow iron oxide nanoparticles.

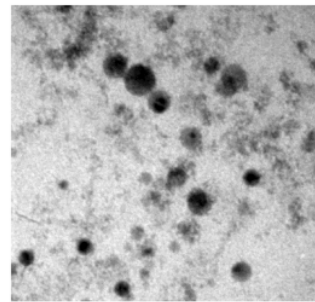


Fig. 9: TEM image of Zn-Fe nanoparticles

The morphology of the colloidal Zn-Fe nanoparticles was obtained by TEM as shown in Fig. 9. Based on these images, it can be seen that most nanoparticles have a spherical shape. The TEM image results were then processed using imageJ software to obtain a histogram of the distribution of Zn-Fe nanoparticles. Figure 10 shows distribution of colloidal Zn-Fe nanoparticles obtained by using the present pulse laser ablation technique. Based on the calculation results, the averaged diameter of the colloidal Zn-Fe nanoparticle mixture is 13 nm.

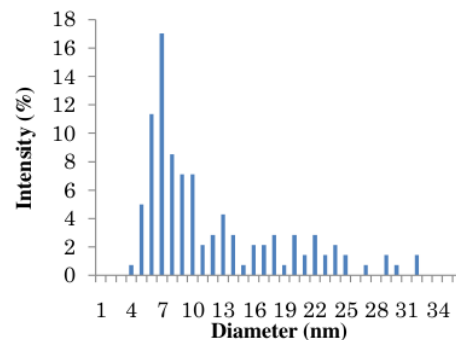


Fig. 10: Size distribution of Zn-Fe nanoparticles.

Furthermore, to determine the bonding of atoms formed from Zn-Fe colloid nanoparticles, an FTIR and XRD analysis was performed. The FTIR spectrum of the mixture is shown in Fig. 11. FTIR spectroscopy shows the position of the ions involved in the crystal lattice through its vibrational mode. The spectrum recorded in the range of wave numbers between 4000 and 400 cm⁻¹. As is seen in the figure, 3434.75 cm⁻¹ band can be related to the O-H stretching vibrations of H₂O absorbed by the sample. The band at 2140 cm⁻¹ is caused by stretching the vibration of the C = H bond. The band at 1656 cm⁻¹ is due to the vibration of the C = O bond. Then the bands 1466 cm⁻¹ and 1321 cm⁻¹ are caused by the vibration of the CH₃ and CH₂ functional groups. The bands which are characteristic of zinc ferrite are located in the range of 540-550 cm⁻¹ and 455-470 cm⁻¹ [17]. In the spectrum bands were detected at 543 cm⁻¹ and 477 cm⁻¹, which are characteristic of zinc ferrite. Shifting the position of the band can occur due to variations in

the bond between the cation-oxygen on the octahedral and tetrahedral sides.

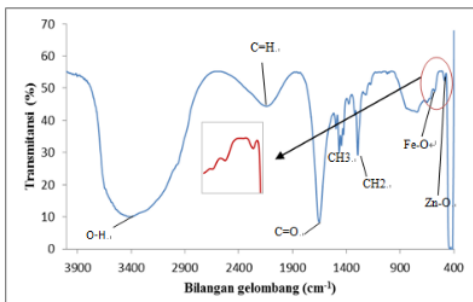


Fig. 11: FTIR spectrum of colloidal Zn-Fe nanoparticles.

XRD analysis was carried out to determine the crystal structure of the mixture of the produced Zn-Fe nanoparticles. For XRD analysis 1 ml of Zn-Fe nanoparticles were dripped on a 1 cm x 1 cm silicon carbide plate and then dried at room temperature for 24 hours. The XRD spectrum of Zn-Fe nanoparticles is shown in Fig. 12.

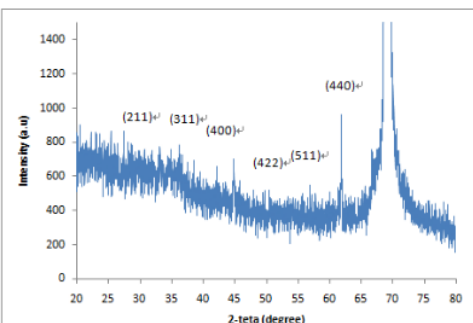


Fig. 12: XRD spectrum of colloidal Zn-Fe nanoparticles.

It can clearly be seen that the diffraction peaks occur at some 2θ of 29.9° , 35.2° , 42.8° , 53.0° , 56.6° , and 62.1° , which represent the lattice constant of (220), (311), (400), (422), (511) dan (440) corresponding to characteristics of ZnFe_2O_4 [15].

3.4. In vitro study of Zn-Fe Nanoparticles as an MRI Contrast Agent

The Zn-Fe nanoparticles produced in this study was then evaluated as a contrast agent in MRI via in-vitro studies. To this end, Zn-Fe nanoparticles in PVP medium were diluted using distilled water with concentrations of 0.156 mM, 0.313 mM, 0.625 mM and 1.25 mM. Nanoparticles with varying concentrations were then inserted into 2 ml vial tubes. The vial tubes containing Zn-Fe nanoparticles are arranged in such a way in an MRI plane. Apart from that, a vial tube containing distilled water was used as a comparison.

To test Zn-Fe nanoparticles as an MRI contrast agent, a scan was performed to obtain T1-weighted and T2-weighted images. T1-weighted MRI images were obtained by spin-echo sequence, with variations of TR 536 and TE 12 ms. T2-weighted images were obtained by spin-echo sequences with TR variations of 2000 and TE of 100 ms. T1-

weighted and T2-weighted images for each variation of nanoparticle concentration are shown in Table 1. It can be observed that the image of dark water in the T1-weighted image for TR and TE is short. In T2-weighted images, water will appear very bright with the old TR and TE settings. The image was then processed with imageJ software to calculate the signal intensity of each sample. The signal intensity value obtained was then used to calculate important variables that determine the image quality, namely contrast enhancement (Cenh) and Signal-to-noise ratio (SNR). Graphs of Cenh and SNR values in T1-weighted and T2-weighted images for variations in sample concentration are shown in Figs. 12 and 13, respectively.

Based on the results of the Cenh calculation, an increment in contrast happens in the T1-weighted and T2-weighted images. This shows that the Zn-Fe nanoparticles produced in the study can be used as contrast agents in T1-weighted and T2-weighted images. The highest contrast increment was obtained at a concentration of 1.25 mM with an increment of 64.26% for T1-weighted images and 81.52% for T2-weighted images. Zn-Fe nanoparticles synthesized in this study provide improved contrast in T2-weighted images, in accordance with previous studies of Zn-Fe nanoparticles suitable for use as MRI T2 image contrast agents (Barcena, 2008; Hoque, 2016). The SNR calculation shows that the SNR at T1-weighted increases with increment of Zn-Fe nanoparticle concentration, while the SNR at T2-weighted decreases with the increment of nanoparticle concentration. The highest SNR at T1-weighted was obtained with the concentration of 1.25 mM, while at T2-weighted the highest was 0.156 mM.

5. Conclusion

Synthesis of colloidal zinc oxide, iron oxide, and Zn-Fe nanoparticles has been successfully carried out by using pulse laser ablation method utilizing a pulse Nd:YAG laser with a laser energy of 35 mJ and a repetition rate of 10 Hz. The results confirmed that all nanoparticles have a spherical shape. The colloidal nanoparticles of zinc oxide, iron oxide, and Zn-Fe have transparent, reddish, and orange colors, respectively. The averaged diameter of the colloidal Zn-Fe nanoparticle mixture is 13 nm. Based on the results of the Cenh calculation, an increment in contrast happens in the T1-weighted and T2-weighted images. This shows that the Zn-Fe nanoparticles produced in the study can be used as contrast agents in T1-weighted and T2-weighted images.

Acknowledgment

This study was financially supported by Ministry of Research, Technology, and Higher Education under the project contract No. 101-122/UN7.P4.3/PP/2019.

References

- [1] D. Yoo, J. H. Lee, T. H. Shin, and J. W. Cheon, Theranostic Magnetic Nanoparticles 44 (2011).
- [2] J. S. Choi, J. H. Lee, T. H. Shin, H. T. Song, E. Y. Kim, and J. Cheon, Self-Confirming "AND" Logic Nanoparticles for Four-Free MRI, J. American Chem. Soc. 132 11015 (2010).
- [3] D. Niu, X. Luo, Y. Li, X. Liu, X. Wang, and J. Shi,

- Manganese-loaded Dual-Mesoporous Silica Spheres for Efficient T1 and T2-Weighted Dual Mode Magnetic Resonance Imaging, *ACS Appl. Mater. Inter.*, **5** 9942-9948 (2013).
- [4] N. Naseri, A. Elham, F. Asgari, and Y. P. Soltanahmadi, An Update on Nanoparticle-based Contrast Agents in Medical Imaging, Artificial Cell, Nanomedicine, and Biotechnology (2017).
- [5] M. Rogosnitzky, and S. Branch, Gadolinium-based Contrast Agent Toxicity: a Review of Known and Proposed Mechanism, *Biometals*, **29** 365-376 (2016).
- [6] T. Tsuzuki, F. Schaffel, M. Muroi, and P.G. McCormick, Magnetic Properties of Mechanochemically Synthesized γ -Fe₂O₃ Nanoparticles, *J Alloy. Compd.*, **509** 5420-5425 (2011).
- [7] Z. Liao, H. Wang, X. Wang, C. Wang, X. Hu, X. Cao, and J. Chang, Biocompatible Surfactin-stabilized Superparamagnetic Iron Oxide Nanoparticles as Contrast Agent for Magnetic Resonance Imaging, *Colloids Surface A*, **370** 1-5 (2010).
- [8] A. Alipour, Z. Soran-Erdem, M. Utkur, V. J. Shamra, O. Algin, E. Saritas, dan H. V. Demir, A new of Cubic SPIONs as Dual-Mode T1 and T2 Contrast Agent for MRI, *Magn. Reson. Imaging*, **49** 16-24 (2017).
- [9] S. M. Hoque, M. S. Hossain, S. Chodhury, S. Akhter, and F. Hyder, Synthesis and Characterization on Zn-Fe Nanoparticles and Its Biomedical Applications, *Material Letter*, **1** 162 60-63 (2016).
- [10] M. M. A. Sinthiya, K. Ramamurthi, S. Mathuri, T. Tanimozhi, N. Kumaresn, M. M. Margoni, and P. C. Karthika, Synthesis of Zinc Ferrite (Zn-Fe) Nanoparticles with Different Capping Agents, *Interntional Journal of ChemTech Research*, **7** 5 2144-2149 (2014).
- [11] A. K. Arora, Ritu, and P. Kumar, A Simple and Effective Synthesis of Nanosized Zn-Fe, *Asian Journal of Chemistry*, **25** 13 7283-7286 (2013).
- [12] R. Rameshabu, R. Ramesh, A. Karthigeyan, and S. Ponnusamy, Synthesis and Propertias of Zn-Fe Nanoparticles by Combustion Methods, *Asian J. Chem.*, **25** (2013).
- [13] M. Ganjali, P. Vahdatkhah, and S. M. B. Marashi, Synthesis of Ni Nanoparticles by Pulsed Laser Ablation Method in Liquid Phase, *Procedia Materials Science*, **11** 359 - 363 (2015).
- [14] S. Wu, P. Wang, Y. Cai, D. Liang, Y. Ye, Z. Tian, J. Liu, and C. Liang, Reduced Graphene Oxide Anchored Magnetic Zn-FeNanoparticles with Enhanced Visible Light Photocatalytic Activity, *RSC Advances*, DOI: 10.1039/C4RA14587A (2014).
- [15] M. Kim, S. Osone, T. Kim, H. Higashi, and T. Seto, Synthesis of Nanopartilces by Laser Ablation: A Review, *KONA Powder Part. J.*, **34** 80-90 (2017).
- [16] R. Sagayaraj, S. Aravazhi, P. Praveen, and G. Ghandrasekaran, Structural, Morphological, and Magnetic Characters of PVP Coated Zn-FeNanoparticles, *J Mater. Sci.-Mater. El.*, **29** 2151-2158 (2018).

Synthesis of Zn-Fe Nanoparticles Using Pulse Laser Ablation as a Contrast Agent in Magnetic Resonance Imaging

ORIGINALITY REPORT



PRIMARY SOURCES

- | | | |
|---|--|-----|
| 1 | Ana Qona'ah, Iis Nurhasanah, Ali Khumaeni.
"Synthesis of Tin Oxide Nanoparticles by Pulsed Laser Ablation Method Using Low-Energy Nd: YAG Laser as an Antibacterial Agent", Journal of Nano Research, 2021
Publication | 4% |
| 2 | C M Satriyani, A Khumaeni. "Synthesis of colloidal copper nanoparticles using pulse laser ablation method", Journal of Physics: Conference Series, 2019
Publication | 2% |
| 3 | aip.scitation.org
Internet Source | 1 % |
| 4 | Szpak, Agnieszka, Sylwia Fiejdasz, Witold Prendota, Tomasz Strączek, Czesław Kapusta, Janusz Szmyd, Maria Nowakowska, and Szczepan Zapotoczny. "T1-T2 Dual-modal MRI contrast agents based on superparamagnetic iron oxide nanoparticles with surface attached | 1 % |

gadolinium complexes", Journal of Nanoparticle Research, 2014.

Publication

-
- 5 Submitted to Universitas Diponegoro 1 %
Student Paper
-
- 6 coek.info 1 %
Internet Source
-
- 7 pubs.rsc.org 1 %
Internet Source
-
- 8 pubs.acs.org 1 %
Internet Source
-
- 9 R. Sagayaraj, S. Aravazhi, P. Praveen, G. Chandrasekaran. "Structural, morphological and magnetic characters of PVP coated ZnFe₂O₄ nanoparticles", Journal of Materials Science: Materials in Electronics, 2017
Publication
-
- 10 Caner Hasirci, Oznur Karaagac, Hakan Köçkar. "Superparamagnetic zinc ferrite: A correlation between high magnetizations and nanoparticle sizes as a function of reaction time via hydrothermal process", Journal of Magnetism and Magnetic Materials, 2018
Publication
-
- 11 Tamar Gordon, Benny Perlstein, Ofir Houbara, Israel Felner, Ehud Banin, Shlomo Margel. "Synthesis and characterization of zinc/iron <1 %

oxide composite nanoparticles and their antibacterial properties", *Colloids and Surfaces A: Physicochemical and Engineering Aspects*, 2011

Publication

12

digitalarchive.gsu.edu

Internet Source

<1 %

13

Hiroyuki Usui, Takeshi Sasaki, Naoto Koshizaki. "Optical Transmittance of Indium Tin Oxide Nanoparticles Prepared by Laser-Induced Fragmentation in Water", *The Journal of Physical Chemistry B*, 2006

Publication

<1 %

14

Reza Massudi. "Environment effect on structure, size control and stability of Zn and ZnO nanoparticles", 2007 7th IEEE Conference on Nanotechnology (IEEE NANO), 08/2007

Publication

<1 %

15

Submitted to University of Puget Sound

Student Paper

<1 %

16

Kefyalew Dagnew Addisu, Balkew Zewge Hailemeskel, Shewaye Lakew Mekuria, Abegaz Tizazu Andrgie, Yu-Chun Lin, Hsieh-Chih Tsai. "Bioinspired, Manganese-Chelated Alginate-Poly(Dopamine) Nanomaterials for Efficient In Vivo T1-Weighted Magnetic Resonance Imaging (MRI)", *ACS Applied Materials & Interfaces*, 2017

<1 %

- 17 www.tandfonline.com <1 %
Internet Source
- 18 Deng, Xiaoran, Yunlu Dai, Jianhua Liu, Ying Zhou, Ping'an Ma, Ziyong Cheng, Yinyin Chen, Kerong Deng, Xuejiao Li, Zhiyao Hou, Chunxia Li, and Jun Lin. "Multifunctional hollow CaF₂:Yb³⁺/Er³⁺/Mn²⁺-poly(2-Aminoethyl methacrylate) microspheres for Pt(IV) pro-drug delivery and tri-modal imaging", *Biomaterials*, 2015.
Publication
- 19 dehesa.unex.es <1 %
Internet Source
- 20 iptek.its.ac.id <1 %
Internet Source
- 21 www.intechopen.com <1 %
Internet Source
- 22 Dipanjan Pan. "Nanomedicine strategies for molecular targets with MRI and optical imaging", *Future Medicinal Chemistry*, 03/2010 <1 %
Publication
- 23 shodhganga.inflibnet.ac.in <1 %
Internet Source

- 24 A Bagaskara, Q M B Soesanto, H Sugito, A Khumaeni. "Effects of repetition rate on the identification of elements in gemstone using the LIBS method", Journal of Physics: Conference Series, 2020 <1 %
Publication
-
- 25 Ali Khumaeni, Wahyu Setia Budi, Koo Hendrik Kurniawan, Kazuyoshi Kurihara. "Metal powder-assisted laser induced breakdown spectroscopy (LIBS) using pulse CO₂ laser for liquid analysis", Journal of King Saud University - Science, 2022 <1 %
Publication
-
- 26 Kyuseok Song, Yong-Il Lee, Joseph Sneddon. "RECENT DEVELOPMENTS IN INSTRUMENTATION FOR LASER INDUCED BREAKDOWN SPECTROSCOPY", Applied Spectroscopy Reviews, 2007 <1 %
Publication
-
- 27 Nashaat Nassar. "Preparation of iron oxide nanoparticles from FeCl₃ solid powder using microemulsions", physica status solidi (a), 05/2006 <1 %
Publication
-
- 28 V. Sri Priyanka, M. K. Murali, M. Abdur Rahman. "Biocidal Properties of Zinc Oxide-Titanium Dioxide-Graphene Oxide" <1 %

Nanocomposites via One-Pot Facile Precipitation Method", BioNanoScience, 2021

Publication

-
- 29 jurnal.ugm.ac.id <1 %
Internet Source
-
- 30 oam-rc.inoe.ro <1 %
Internet Source
-
- 31 vdoc.pub <1 %
Internet Source
-
- 32 www.ncbi.nlm.nih.gov <1 %
Internet Source
-
- 33 "Green Metal Nanoparticles", Wiley, 2018 <1 %
Publication
-
- 34 Ichsan Nur Lintang, Iis Nurhasanah, Ali Khumaeni. "Synthesis of gadolinium nanoparticles using pulsed laser ablation method", AIP Publishing, 2019 <1 %
Publication
-
- 35 Springer Series in Biomaterials Science and Engineering, 2016. <1 %
Publication
-
- 36 Wang, Xia, Dechao Niu, Qing Wu, Song Bao, Teng Su, Xiaohang Liu, Shengjian Zhang, and Qigang Wang. "Iron oxide/manganese oxide co-loaded hybrid nanogels as pH-responsive <1 %

magnetic resonance contrast agents",

Biomaterials, 2015.

Publication

37 hdl.handle.net <1 %

Internet Source

38 Byung Hyo Kim, Nohyun Lee, Hyoungsu Kim, Kwangjin An et al. " Large-Scale Synthesis of Uniform and Extremely Small-Sized Iron Oxide Nanoparticles for High-Resolution Magnetic Resonance Imaging Contrast Agents ", Journal of the American Chemical Society, 2011 <1 %

Publication

39 S Avicenna, I Nurhasanah, A Khumaeni. <1 %

"Synthesis of gadolinium nanoparticles in spinach-extracted liquid using a pulse laser ablation method", Journal of Physics: Conference Series, 2020

Publication

40 Victoriya Zheltova, Anna Vlasova, Natalia Bobrysheva, Ilgiz Abdullin et al. "Fe₃O₄@HAp core-shell nanoparticles as MRI contrast agent: Synthesis, characterization and theoretical and experimental study of shell impact on magnetic properties", Applied Surface Science, 2020 <1 %

Publication

Exclude quotes Off

Exclude bibliography On

Exclude matches Off

Synthesis of Zn-Fe Nanoparticles Using Pulse Laser Ablation as a Contrast Agent in Magnetic Resonance Imaging

GRADEMARK REPORT

FINAL GRADE

/0

GENERAL COMMENTS

Instructor

PAGE 1

PAGE 2

PAGE 3

PAGE 4

PAGE 5

PAGE 6
